DESIGN AND CONTROL OF STANDALONE PHOTOVOLTAIC SYSTEMS

By

Said El-Barbari*; Frank N. Okafor, M*IEEE* and W. Hofmann*, M*IEEE***

*

** Department of Electrical and Electronic Engineering,
University of Lagos, Akoka.

1.0 ABSTRACT

The design philosophy for a stand alone photovoltaic system supplying an AC load is to provide symmetrical three phase voltages with constant frequency and amplitude. This is often achieved through the introduction of a fourth leg to the usual three phase inverter, which presents severe challenges in both analysis and implementation. In this paper a control strategy incorporating a reduced order disturbance observer and feed forward disturbance canceling in the state space is presented. Simulation results for balanced and unbalanced load show stable dynamic performance of the amplitude and frequency profiles of the output voltage. Experimental results further authenticate the proposed control technique.

Key words: *stand alone photovoltaic systems, disturbance canceling, reduced order observer, digital control.*

2.0 INTRODUCTION

Most developing countries of Africa and Asia are usually characterized by small pockets of settlements which are remote from the cities. With regards to power supply to these communities, economic considerations clearly indicate that grid connection is not viable.

Consequently, photovoltaic systems either as stand alone or highbred with other systems have been canvassed as a viable option [1,2]. However, the design of stand alone photovoltaic systems supplying AC loads presents severe challenges in both analysis and implementation. A fourth leg has to be introduced to the usual three leg inverter to form the so called 4-leg inverter system which functions to ensure a balanced three phase load. The control of this inverter is the subject matter of this paper.

In principle, the task of a four leg Voltage Source Inverter (VSI) for standalone photovoltaic systems is to produce symmetrical three phase sinusoidal voltages from a DC voltage source, so that three and single phase loads can be supplied with AC voltage with constant amplitude and frequency. Unfortunately the consumer in a standalone power supply net may be unknown and here underlies an arbitrary load profile. In the worst case the load profile represents switching on or off at full load. In a photovoltaic standalone power supply net the consumer could be three as well as single phase. Therefore, a neutral connection is needed to control each phase voltage independently. Different topologies to realize the neutral connection are discussed in [6]. The generation of the neutral connection using a fourth leg is advantageous because a smaller DC link capacitor can be used and a modulation grad of 1.16 can be theoretically reached when using the three dimensional space vector modulation method [4]. From the control point of view, the load current represents a disturbance which affects both the output voltage and the inductance current of the output filter.

In the technical literature, a number of strategies for controlling such a system has been presented [8, 9, 10, 11]. One thing unique about the listed approaches is that they are applicable to situations of symmetrical load. In [3], an unbalanced load is considered by introducing a major voltage control loop and a minor current loop. Both feedback loops deploy a PI-regulator in the rotating dqo coordinate. Because the load is unbalanced, an additional loop for the o-sequence current and voltage must be implemented to ensure

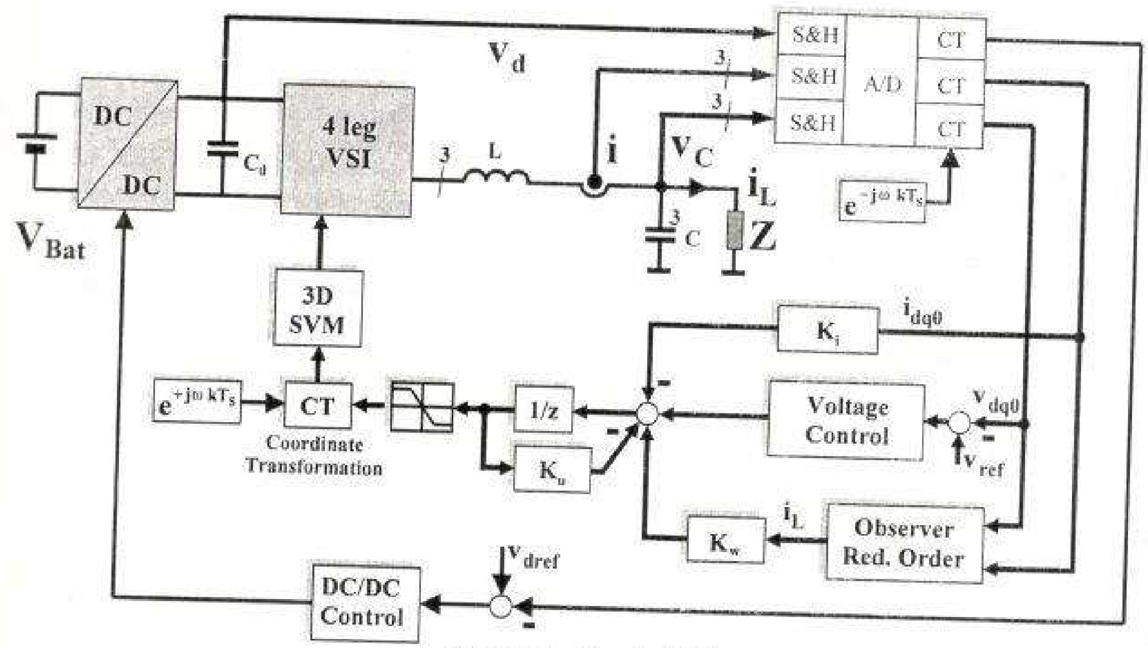

Figure 1: Control Strategy

symmetry. This approach has been applied to the control of UPS systems [11]. Its major advantage is simplicity of implementation, especially in the analog domain. Major constraints in the digital domain are the computation time and sampling rate.

It is well known that micro-controllers have relatively high calculation time and slow analog to Digital (AD) converters. Hence implementation PI-control for a four-leg VSI on such a microcontroller will fail to achieve output voltage symmetry for an unbalanced load. This is because, the d, q and o-component of the output voltage contain additional oscillating quantities. In consequence, the PIregulation can only cause a phase shift without canceling the error completely. Furthermore, the long computation time will introduce a non-negligible deadtime which impacts negatively on overall system stability.

This paper adopts an approach which eliminates or mitigates against the above disadvantages. Both feed forward disturbance canceling and a reduced order disturbance observer are incorporated in the state space model while a three dimensional space, vector modulation is applied to the four-leg inverter. The result is a higher utilization of the DC-link voltage and the elimination of the load current measuring devices which is now estimated by the observer. The efficacy of the proposed technique is illustrated using simulation and experimental results.

This paper is organized as follows: Section II presents the philosophy of the proposed control approach while the 4-leg VSI formulation is discussed in Section III. Extensions of the model to include the load current and the reduced order observer are described in Sections IV and V respectively while the disturbance decoupling and its cancellation using a feedforward controller are explained successively in sections VI and VII. The strategy for voltage control is outlined in section VIII while simulation and experimental results are presented in sections IX and X respectively, only to be followed by the concluding remarks in section XI.

3.0 PROPOSED CONTROL

As stated above, the main control burden is to maintain constant amplitude and frequency of the output voltage. This should remain so irrespective of the load parameter and asymmetry factor. The secondary control objective is to keep the DC link voltage constant and to protect the inverter from over current. Figure 1 illustrates the block diagram of the control strategy. For the main objective of the control the three capacitor voltages and inductance currents are measured. For the secondary objective of the control the DC link voltage is measured. Because, The AD converter on the microcontroller works in a multiplex manner, a sample and hold unit is used to get the digital values of the measured voltages and currents at the same time. The whole conversion time is 70ms. As the output voltage is sinusoidal, the use of a conventional PI- controller will discard, because the I-fraction will not guarantee stationary precision, otherwise it will only cause a phase shift. For this reason the control is designed in the rotating dq0 coordinate. The phase voltages and currents are multiplied by the complex operator e-jwkTs, with the result that ac quantities will become dc quantities which can be regulated with a PI-control.

Afterwards the transformed phase voltages are compared with the reference value and the error signal is led to the voltage PI-controller. The transformed phase currents are fed back using the stat feedback matrix Ki. In this way the eigenvalues of the close loop plant will be shifted to an appropriate place in the z-plant,to enhance the stability reserve and system dynamic. The calculation of the control algorithm in the microcontroller leads to a time delay of one sampling period. This is presented by the block 1/z, where z is the discrete shift operator. The delayed control signal can be regarded as a state space variable and thus can be fed back through the feed back matrix Ku. The control signal will then be bounded to realize the over current protection. After that the control signal is transformed to the stationary coordinate of the output voltage by multiplying with the complex vector ejwkTs. The three dimensional Space Vector Modulator (3D SVM) generate the switching signals of the power transistor of the four leg VSI. The control of the DC link voltage is realised with a PI-regulator. The control signal represents the duty cycle for the boost converter to ensure a constant DC link voltage.

As long as the load is symmetrical, the PI-regulator is able to fulfill the demands of the major objective. If the load is unsymmetrical, the output voltage is composed of positive, negative and zero sequence. The negative sequence in the rotating dq0-coordinate oscillates with the double frequency of the output voltage. As the sampling rate is relatively low (333ms), the PI regulator will suffer from a velocity error and will not be able to compensate the disturbance completely. This problem can be solved by feeding forward the load currents which act as a disturbance on the plant. In the proposed system, the load currents will not be measured, therefore a disturbance model and an observer reduced order are used to estimate the load currents. The matrix Kw is used to feed forward the estimated load currents to the output of the voltage control loop.

4.0 VOLTAGE SOURCE INVERTER MODEL

The topology of this inverter is shown in figure 2. One can recognise the three standard legs and the additional 4^{th} leg. In this case the star point of the load and the output filter is connected to the 4^{th} leg. A boost converter is connected to the DC link to realise an operating DC link voltage of 650V. Neglecting the inverter losses, each inverter leg can be modelled as an ideal switch s, which can be either s=1, if the upper power transistor is on and the lower one is off, or s=1, if the upper on is off and the lower one is on. In this case the load underlies either the positive p or negative n potential of the DC link.

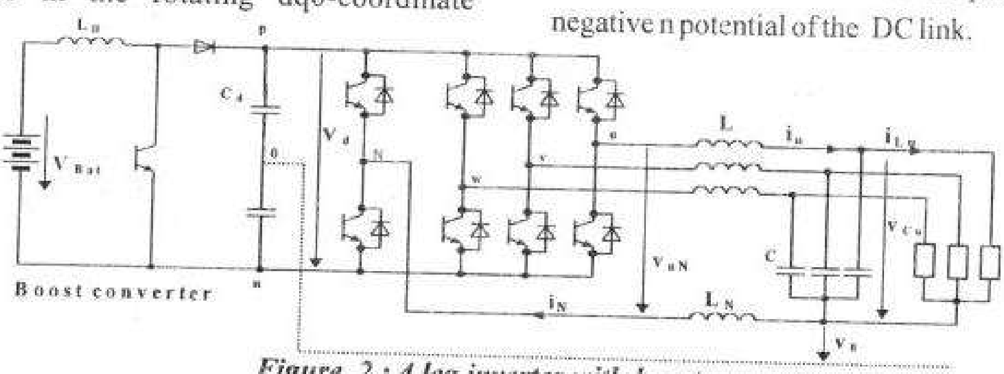

Figure. 2 : 4 leg inverter with boost converter

The control signal generated in the microcontroller represents the voltage mean value between each phase and the neutral leg N. The three dimensional space vector modulator converts these control signals to 4 switching signals for each leg.

$$v_{xN} = v_{x0} - v_{N0} = \frac{V_d}{2} d_x$$

where $d_x \in \{1,-1\}$ is the mean value of the control signal.

$$v_{xN} = L\frac{di_x}{dt} + i_x R_L + v_{Cx} - L_N \frac{di_N}{dt} - i_N R_{LN}, x = u, v, w$$

The phase currents can be written as:

$$i_x = C\frac{dv_{Cx}}{dt} + \frac{v_{Cx}}{R_c} + i_{Lx} \text{ and}$$

$$i_N = -\sum_x i_x, \quad x = u, v, w$$

Defining

$$L_{mu} = \begin{pmatrix} L_N + L & L_N & L_N \\ L_N & L_N + L & L_N \\ L_N & L_N & L_N + L \end{pmatrix} \text{ and}$$

$$R_{mu} = \begin{pmatrix} (R_L + R_{LN}) & R_{LN} & R_{LN} \\ R_{LN} & (R_L + R_{LN}) & R_{LN} \\ R_{LN} & R_{LN} & (R_L + R_{LN}) \end{pmatrix}$$

The differential equations of the voltages and currents of the 4 leg inverter can be represented as the following:

$$\frac{d}{dt}\begin{pmatrix} v_{Cu} \\ v_{Cv} \\ v_{Cw} \end{pmatrix} = -\frac{1}{R_c C}\begin{pmatrix} v_{Cu} \\ v_{Cv} \\ v_{Cw} \end{pmatrix} + \frac{1}{C}\begin{pmatrix} i_u \\ i_v \\ i_w \end{pmatrix} - \frac{1}{C}\begin{pmatrix} i_{Lu} \\ i_{Lv} \\ i_{Lw} \end{pmatrix}$$

$$\frac{d}{dt}\begin{pmatrix} i_u \\ i_v \\ i_w \end{pmatrix} = -L_{mu}^{-1}\begin{pmatrix} v_{Cu} \\ v_{Cv} \\ v_{Cw} \end{pmatrix} - L_{mu}^{-1} R_{mu}\begin{pmatrix} i_u \\ i_v \\ i_w \end{pmatrix} + L_{mu}^{-1}\begin{pmatrix} v_{uN} \\ v_{vN} \\ v_{wN} \end{pmatrix} \quad (10)$$

with

$$\bar{\mathbf{v}}_C = \begin{pmatrix} v_{Cu} \\ v_{Cv} \\ v_{Cw} \end{pmatrix}, \bar{\mathbf{i}} = \begin{pmatrix} i_u \\ i_v \\ i_w \end{pmatrix}, \bar{\mathbf{i}}_L = \begin{pmatrix} i_{Lu} \\ i_{Lv} \\ i_{Lw} \end{pmatrix},$$

(3) $$\bar{\mathbf{v}}_{xN} = \begin{pmatrix} v_{uN} \\ v_{vN} \\ v_{wN} \end{pmatrix} = \frac{V_d}{2}\begin{pmatrix} d_u \\ d_v \\ d_w \end{pmatrix}$$

and

(4) $$\mathbf{A}_{C11} = -\frac{1}{R_c C}\begin{pmatrix} 1 & 0 & 0 \\ 0 & 1 & 0 \\ 0 & 0 & 1 \end{pmatrix}, \mathbf{A}_{C12} = \frac{1}{C}\begin{pmatrix} 1 & 0 & 0 \\ 0 & 1 & 0 \\ 0 & 0 & 1 \end{pmatrix},$$

$$\mathbf{A}_{C21} = -L_{mu}^{-1}, \mathbf{A}_{C22} = -L_{mu}^{-1} R_{mu}$$

(5) $$\mathbf{B}_{C11} = -\frac{1}{C}\begin{pmatrix} 1 & 0 & 0 \\ 0 & 1 & 0 \\ 0 & 0 & 1 \end{pmatrix}, \mathbf{B}_{C22} = L_{mu}^{-1},$$

(6)

The brief form of the above equations is:

$$\frac{d}{dt}\begin{pmatrix} \bar{\mathbf{v}}_C \\ \bar{\mathbf{i}} \end{pmatrix} = \begin{pmatrix} \mathbf{A}_{C11} & \mathbf{A}_{C12} \\ \mathbf{A}_{C21} & \mathbf{A}_{C22} \end{pmatrix}\begin{pmatrix} \bar{\mathbf{v}}_C \\ \bar{\mathbf{i}} \end{pmatrix} + \begin{pmatrix} 0 \\ \mathbf{B}_{C22} \end{pmatrix}\bar{\mathbf{v}}_{xN} + \begin{pmatrix} \mathbf{B}_{C11} \\ 0 \end{pmatrix}\bar{\mathbf{i}}_L \quad (11)$$

(7)

$$\bar{\mathbf{y}}_t = \begin{pmatrix} \bar{\mathbf{v}}_C \\ \bar{\mathbf{i}} \end{pmatrix} \quad (12)$$

From the state space representation (11) and (8) (12) it is obvious that the disturbance $\mathbf{i}_L$ directly affects the output voltage and indirectly the output current. Using simulation tools such as MATLAB and considering a time delay of one sampling period, the discrete state space plant model of the 4 leg VSI in the rotating dq0-coordinat can be written as:

(9)

$$\begin{pmatrix} \mathbf{v}_{C(k+1)} \\ \mathbf{i}_{(k+1)} \end{pmatrix} = \begin{pmatrix} \mathbf{A}_{d11} & \mathbf{A}_{d12} \\ \mathbf{A}_{d21} & \mathbf{A}_{d22} \end{pmatrix}\begin{pmatrix} \mathbf{v}_{C(k)} \\ \mathbf{i}_{(k)} \end{pmatrix} + \begin{pmatrix} \mathbf{B}_{d1} \\ \mathbf{B}_{d2} \end{pmatrix}\mathbf{d}_{(k-1)} + \begin{pmatrix} \mathbf{E}_{d1} \\ \mathbf{E}_{d2} \end{pmatrix}\mathbf{i}_{L(k)} \quad (13)$$

$$\mathbf{y}_{(k)} = \begin{pmatrix} \mathbf{v}_{C(k)} \\ \mathbf{i}_{(k)} \end{pmatrix} \quad (14)$$

Where $\mathbf{d}$ is the normalised control vector. The delayed control vector $\mathbf{d}$ in (13) can be regarded as

a state space variable. so that equ. (13) can be written in the following form.

$$\begin{pmatrix} \mathbf{v}_{C(k+1)} \\ \mathbf{i}_{(k+1)} \\ \mathbf{d}_{(k)} \end{pmatrix} = \begin{pmatrix} \mathbf{A}_{d11} & \mathbf{A}_{d12} & \mathbf{B}_{d1} \\ \mathbf{A}_{d21} & \mathbf{A}_{d22} & \mathbf{B}_{d2} \\ \mathbf{0} & \mathbf{0} & \mathbf{0} \end{pmatrix} \begin{pmatrix} \mathbf{v}_{C(k)} \\ \mathbf{i}_{(k)} \\ \mathbf{d}_{(k-1)} \end{pmatrix} + \begin{pmatrix} \mathbf{0} \\ \mathbf{0} \\ \mathbf{I} \end{pmatrix} \mathbf{d}_{(k)} + \begin{pmatrix} \mathbf{E}_{d1} \\ \mathbf{E}_{d2} \\ \mathbf{0} \end{pmatrix} \mathbf{i}_{L(k)}$$

$$\mathbf{y}_{(k)} = \begin{pmatrix} \mathbf{I} & \mathbf{0} & \mathbf{0} \\ \mathbf{0} & \mathbf{I} & \mathbf{0} \end{pmatrix} \begin{pmatrix} \mathbf{v}_{C(k)} \\ \mathbf{i}_{(k)} \\ \mathbf{d}_{(k-1)} \end{pmatrix}$$

The standard short form representation of the discrete state space plant model is as follows:

$$\mathbf{x}_{k+1} = \mathbf{A}\mathbf{x}_k + \mathbf{B}\mathbf{u}_k + \mathbf{E}\mathbf{z}_k$$

$$\mathbf{y}_k = \mathbf{C}\mathbf{x}_k$$

with

$$\mathbf{A} = \begin{pmatrix} \mathbf{A}_{d11} & \mathbf{A}_{d12} & \mathbf{B}_{d1} \\ \mathbf{A}_{d21} & \mathbf{A}_{d22} & \mathbf{B}_{d2} \\ \mathbf{0} & \mathbf{0} & \mathbf{0} \end{pmatrix}, \mathbf{B} = \begin{pmatrix} \mathbf{0} \\ \mathbf{0} \\ \mathbf{I} \end{pmatrix}, \mathbf{E} = \begin{pmatrix} \mathbf{E}_{d1} \\ \mathbf{E}_{d2} \\ \mathbf{0} \end{pmatrix},$$

$$\mathbf{x}_k = \begin{pmatrix} \mathbf{v}_{C(k)} \\ \mathbf{i}_{(k)} \\ \mathbf{d}_{(k-1)} \end{pmatrix}$$

$$\mathbf{C} = \begin{pmatrix} \mathbf{I} & \mathbf{0} & \mathbf{0} \\ \mathbf{0} & \mathbf{I} & \mathbf{0} \end{pmatrix}, \mathbf{u}_k = \mathbf{d}_k \text{ and } \mathbf{z}_k = \mathbf{i}_{L(k)}.$$

5. MODEL OF THE LOAD CURRENT

To reconstruct the load currents, an exact knowledge is necessary about the properties of the load current track in the dq0-coordinate. If the load is balanced, the d- and q-component are DC quantities and the 0-component is zero.

If the load is unbalanced both the d- and q-component contain an additional AC quantity, that oscillates with the double frequency of the output voltage.

The 0-component is not equal zero and oscillates with the same frequency as the output voltage. The phase shift between the AC quantities of the d- and q-axis is 90°.

According to this knowledge, the load current can be represented as differential equations. The load current discrete state space model (15) can be written as follows:

$$\tilde{\mathbf{x}}_{k+1} = \tilde{\mathbf{A}}\tilde{\mathbf{x}}_k \tag{19}$$

$$\mathbf{z}_k = \tilde{\mathbf{C}}\tilde{\mathbf{x}}_k \tag{20}$$

(16)

with

$$\tilde{\mathbf{A}} = \begin{pmatrix} \cos(2\omega T_S) & \sin(2\omega T_S) & 0 & 0 \\ -\sin(2\omega T_S) & \cos(2\omega T_S) & 0 & 0 \\ 0 & 0 & \cos(\omega T_S) & \sin(\omega T_S) \\ 0 & 0 & -\sin(\omega T_S) & \cos(\omega T_S) \end{pmatrix}$$

and

(17)

$$\tilde{\mathbf{C}} = \begin{pmatrix} 1 & 0 & 0 & 0 \\ 0 & 1 & 0 & 0 \\ 0 & 0 & 1 & 0 \end{pmatrix}$$

(18)

The factor 2 in the system matrix $\tilde{\mathbf{A}}$ indicates the double frequency and the structure of the top sub matrix indicates 90° phase shift between the d- and q-axis of the load current model. The bottom sub matrix is used to model the 0-sequence component of the load current.

6. REDUCED ORDER OBSEVER

The reduced order observer is constructed from the state space model of the plant and load current. Substituting (19-20) in (17-18) The state space model of the 4 leg **VSI** can be expressed as:

$$\begin{pmatrix} \mathbf{x}_{k+1} \\ \tilde{\mathbf{x}}_{k+1} \end{pmatrix} = \begin{pmatrix} \mathbf{A} & \mathbf{E}\tilde{\mathbf{C}} \\ \mathbf{0} & \tilde{\mathbf{A}} \end{pmatrix} \begin{pmatrix} \mathbf{x}_k \\ \tilde{\mathbf{x}}_k \end{pmatrix} + \begin{pmatrix} \mathbf{B} \\ \mathbf{0} \end{pmatrix} \mathbf{u}_k \tag{21}$$

$$\mathbf{y}_k = \begin{pmatrix} \mathbf{C} & \mathbf{0} \end{pmatrix} \begin{pmatrix} \mathbf{x}_k \\ \tilde{\mathbf{x}}_k \end{pmatrix} \tag{22}$$

The reduced order observer equation is:

$$\mathbf{r}_{k+1} = \left(\tilde{\mathbf{A}} - \mathbf{H}\mathbf{E}\tilde{\mathbf{C}}\right)\mathbf{r}_k - \mathbf{H}\mathbf{B}\mathbf{u}_{(k)} + \left(\left(\tilde{\mathbf{A}} - \mathbf{H}\mathbf{E}\tilde{\mathbf{C}}\right)\mathbf{H} - \mathbf{H}\mathbf{A}\right)\hat{\mathbf{y}}_k \tag{23}$$

$$\tilde{\mathbf{x}}_k = \mathbf{r}_k + \mathbf{H}\hat{\mathbf{y}}_k \tag{24}$$

where $\hat{\mathbf{y}}_k = \mathbf{x}_k$ and **H** 4x9 observer matrix.

The implementation of the reduced order observer on the 80c166 is very simple and regarding the calculation time it is fast enough. There are 25 multiplications and 25 additions and they will need about 80us.

7. DECOUPLING THE DISTURBANCE SIGNAL

There are many possibilities to compensate or minimize the effect of the disturbance (disturbance decoupling). Only in special cases, the disturbance is suppressed without taking additional measures. This is the case when all column of the disturbance matrix **E** can be represented as a linear combination of those eigenvectors v of **A** so that $\mathbf{C}v=\mathbf{0}$ Error! Reference source not found.. When such a disturbance decoupling at the output **y** does not exist, one can apply the states feedback low $\mathbf{y}_k=-\mathbf{K}\mathbf{x}_k$ to force this decoupling or at least to minimise the disturbance influence. Another possibility is to feed forward the disturbance. Applying z-transformation to (17) and (18) the output of the plant can be written as:

$$\mathbf{y}(z)=\underbrace{\mathbf{C}(z\mathbf{I}-\mathbf{A})^{-1}\mathbf{B}}_{G_u(z)}\mathbf{u}(z)+\underbrace{\mathbf{C}(z\mathbf{I}-\mathbf{A})^{-1}\mathbf{E}}_{G_z(z)}\mathbf{z}(z) \tag{25}$$

where $\mathbf{G}_u$ the reference transfer function and $\mathbf{G}_z$ the disturbance transfer function of the plant.

Disturbance decoupling is given when

$$\mathbf{u}(z)=-(\mathbf{G}_u(z))^{-1}\mathbf{G}_z(z)\mathbf{z}(z). \tag{26}$$

Equation (26) represents a dynamical disturbance decouplig. Disadvantages can arise concerning the practical implementation and realisation of (26). In addition, it can affect the stability of the plant [10]. That is why the stationary decoupling is more preferred, which is given when the influence of the sum $\mathbf{B}\mathbf{u}_k+\mathbf{E}\mathbf{z}_k$ in equation (17) is minimised by choosing $\mathbf{u}_k=(\mathbf{B}^T\mathbf{B})^{-1}\mathbf{B}^T\mathbf{E}\mathbf{z}_k$. Because of the proximity of this expression the remaining effect of the disturbance is not quantifiable. An alternative is the stationary disturbance feed forward of (26).

$$\mathbf{u}(z)=-(\mathbf{G}_u(1))^{-1}\mathbf{G}_w(1)\mathbf{z}(z) \tag{27}$$

8. FEEDFORWARD DISTURBANCE CONTROL

The disturbance feed forward design rests upon (21-22), in contradictory to (27), can be used for any disturbance model, by applying $\mathbf{u}_k=-\mathbf{K}_w\tilde{\mathbf{x}}_k-\mathbf{K}_x\mathbf{x}_k$, where $\mathbf{K}_x$ the states feedback matrix and $\mathbf{K}_w$ the disturbance model states feed forward matrix. The problem to solve is to find an appropriate matrix $\mathbf{K}_w$ so that the eigenvalues of the disturbance model, in this case the eigenvalues of the matrix $\tilde{\mathrm{A}}$, will be unobservable. For a single eigenvalue λ, this means that $[\mathbf{C}\ \ \mathbf{0}]v=\mathbf{0}$, where v is the eigenvecktor of λ (*Gilbert-criterion*). The feed back matrix $\mathbf{K}_x$ is assumed to be already known and integrated in **A**. This can be easily done by using some pole placement tools like in MATLAB. Assigning the index 1,....,n to the eigenvalues of **A** and n+1,....,n+s to the eigenvaluse of $\tilde{\mathbf{A}}$, the eigenvecktors $v_{n+1},....,v_{n+s}$ can be calculated from the following equation.

$$\begin{pmatrix}\lambda_{n+i}\mathbf{I}-\mathbf{A} & -\mathbf{E}\tilde{\mathbf{C}}+\mathbf{B}\mathbf{K}_w\\ \mathbf{0} & \lambda_{n+i}\mathbf{I}-\tilde{\mathbf{A}}\end{pmatrix}\underbrace{\begin{pmatrix}v_{x,n+i}\\ v_{\tilde{x},n+i}\end{pmatrix}}_{v_{n+i}}=\mathbf{0}\quad ,i=1,....,s$$

and (28)

$$v_{x,n+i}=(\lambda_{n+i}\mathbf{I}-\mathbf{A})^{-1}(\mathbf{E}\tilde{\mathbf{C}}-\mathbf{B}\mathbf{K}_w)v_{\tilde{x},n+i} \tag{29}$$

applying the *Gilbert-criterion* to (29)

$$(\mathbf{C}\ \ \mathbf{0})\begin{pmatrix}v_{x,n+i}\\ v_{\tilde{x},n+i}\end{pmatrix}=\mathbf{C}v_{x,n+i}=\mathbf{0}\quad \text{and} \tag{30}$$

(31)

$$y(z)=\underbrace{C(z1-A)^{-1}B}_{G_u(z)}u(z)+\underbrace{C(z1-A)^{-1}E}_{G_z(z)}z(z)$$

and finally the feed forward matrix can be expressed as:

$$K_u=\left[G_u^{-1}(\lambda_{v+1})G_z(\lambda_{v+1})\tilde{C}v_{\bar{z},v+1}\ldots G_u^{-1}(\lambda_{v+r})G_z(\lambda_{v+r})\tilde{C}v_{\bar{z},v+r}\right]\times\left[v_{\bar{z},v+1}\ldots v_{\bar{z},v+r}\right]^{-1} \quad (32)$$

This method of disturbance decoupling was introduced by B. Lohmann in details in [10].

9. Voltage Control

As mentioned before the states feed back matrix $\mathbf{K}_x$ was chosen in such a way to place the poles of the plant at an appropriate position in z-plane to get fast dynamic performance. Only the currents $\mathbf{i}_{(k)}$ and the delayed control signals $\mathbf{d}_{(k)}$ were fed through this matrix. This was enough to get a stable performance and fast current response of the plant. A PI control was applied to the voltage to guarantee the stationary accuracy and to decouple the d-, q- and 0-axises from each other. The control structure is illustrated in figure 3.

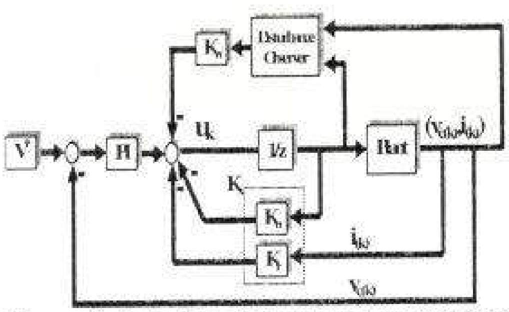

Figure 3: Principle of the voltage control loop with disturbance decoupling

10. Simulation Results

Figure 11 and 12 illustrate the simulation results of the proposed control with and without load current disturbance decoupling for the following load cycle

0.00-0.04s balanced load ($I_{Lu}=I_{Lv}=I_{Lw}=16.3\angle 0$)

0.04-0.08s balanced load ($I_{Lu}=I_{Lv}=I_{Lw}=3.2A\angle 0$)

0.08-0.12s unbalanced load ($I_{Lu}=32.6A\angle 0$, $I_{Lv}=I_{Lw}=3.2A$)

From figure 4 one can see that the PI control alone is only able to compensate the load current disturbance when the load is balanced. That is because the load current positive sequence will be a DC quantity in the synchronised dq0-coordinate. When the load is unbalanced, in addition to the positive sequence, the load current will contain also a a negative sequence, which oscillates with the double frequency of the rotating dq0-cordinate, and a zero-sequence which has the same frequency as the dq0-cordinate. The PI control will not be able to compensate this oscillations completely especially when the sampling frequency is relatively low. From the simulation results one can see the high dynamic performance of the introduced observer based control method as the disturbance of the output voltage is quickly compensated.

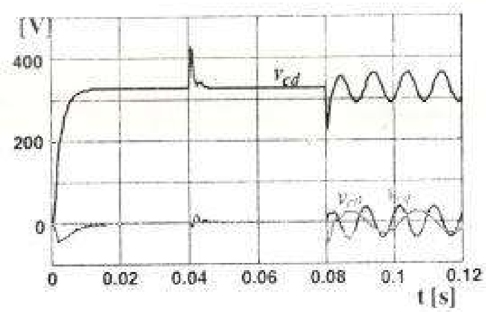

Figure 4: Voltages of the output filter without disturbance decoupling

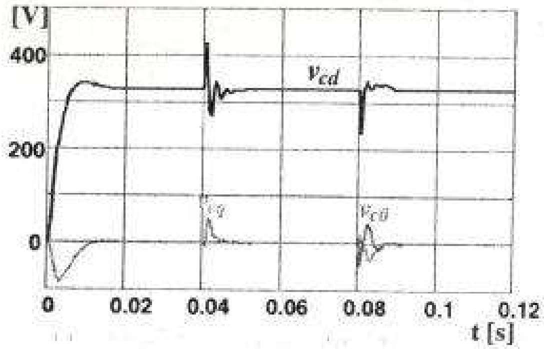

Figure 5 : Voltages of the output filter with disturbance decoupling

The output voltage can be expressed as a superposion of the disturbance transfer function, in this case the load current, and the output voltage reference transfer function. This relation is shown by the following expression:

$$\begin{pmatrix} v_{Cd}(z) \\ v_{Cq}(z) \\ v_{C0}(z) \end{pmatrix} = \begin{pmatrix} G_{zd}(z) & G_{zq}(z) & 0 \\ -G_{zq}(z) & G_{zd}(z) & 0 \\ 0 & 0 & G_{z0}(z) \end{pmatrix} \begin{pmatrix} i_{Ld}(z) \\ i_{Lq}(z) \\ i_{L0}(z) \end{pmatrix} +$$

$$\begin{pmatrix} G_{wd}(z) & G_{wq}(z) & 0 \\ -G_{wq}(z) & G_{wd}(z) & 0 \\ 0 & 0 & G_{w0}(z) \end{pmatrix} \begin{pmatrix} v_d^*(z) \\ v_q^*(z) \\ v_0^*(z) \end{pmatrix} \quad (33)$$

From the above equation the disturbance to output transfer function of the d- and 0-axis of the output voltage are:

$$v_{Cd}(z) = G_{zd}(z) i_{Ld}(z) + G_{zq}(z) i_{Lq}(z) \quad (34)$$

$$v_{C0}(z) = G_{z0}(z) i_{L0}(z) \quad (35)$$

Fig. 6 and 7 show the bode diagram of G_{zd} and G_{zq}.

If the load is balanced the load current in the dq0-coordinate will contain only DC quantities, which have a high dumping at 0(rad/sec). If the load is unbalanced, at the point of intersection, both G_{zd} and G_{zq} has the same magnitude and a relative phase shift to each other of 90°. The intersection point frequency is 100Hz which is the frequency of the negative sequence in the rotating dq0-coordinate. As mentioned in section IV, if the load is unbalanced the relative phase shift between the AC quantities of the d- and q-axis is 90°. This will result in a total phase shift of 180°, and the disturbance at this frequency will be cancelled as can be seen from fig. 6.

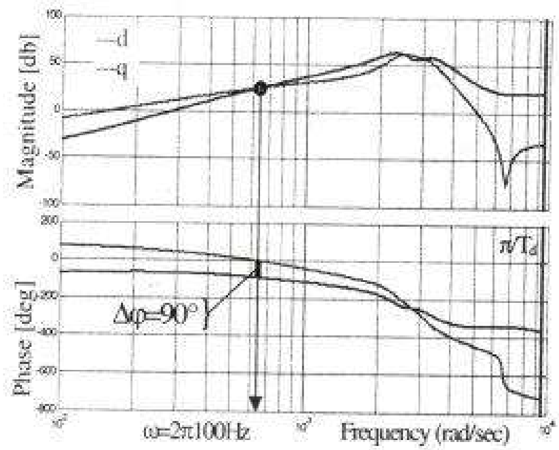

Figure 6 : Bode diagram of the disturbance to output transfer function (d-axis of the output voltage)

The bode diagram of the 0-load current to the output 0-voltage of equation (35) shows at 50Hz a notch filter characteristic, so that any disturbance at this frequency will be highly dumped, as shown in fig.

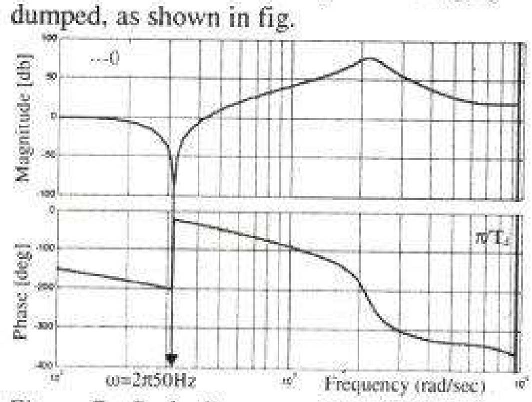

Figure 7: Bode diagram of the disturbance to output transfer function (0-axis of the output voltage)

II. EXPERIMENTAL RESULTS

For experimental purpose five 1200V, 75A IGBT Intelligent power module (IPM) from MITSUBISHI were used. Four IPM half bridges are used to build the four leg inverter and the fifth half bridge to build the boost converter. The output filter was optimised, so that at 9kHz switching frequency the whole inverter losses are minimised [5]. A microcontroller of the type 80C166 from SIEMENS is used to control the whole system. At the output of the microcontroller five PWM signals are generated, one to control the boost converter and four to control the 4 leg inverter. The complimentary of these four signals and the dead time generation was done externally per hardware.

Figure 8 shows the output voltage of the inverter in the rotating dq0-coordinate system, when unbalanced load is applied. As it can be seen from the figure, without observer and disturbance feed forward, the PI-control alone is not able to compensate the disturbance completely. As the q- and 0-component of the output voltage supposed to be zero and the d-component a constant DC quantity. Figure 9 shows the output voltage when the observer and the disturbance feed forward is switched on. As

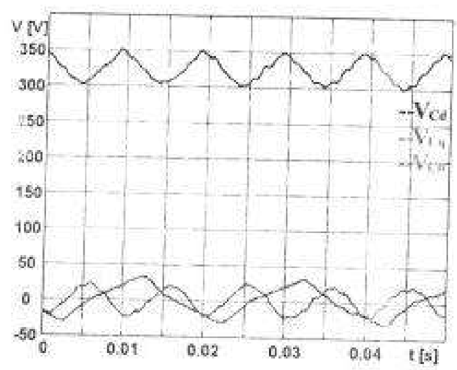

Fig. 8 measured output voltage without observer (single phase ohmic load of 5A

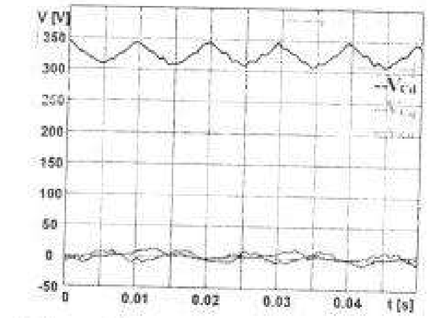

Figure 9: measured output voltage with observer

it can be seen from the figure, the output voltage tracking is highly improved.

However, an error still exist due to the inaccurate measurements and fixed-point number implementation of the control algorithm on the microcontroller, so that the point of intersection of the d- and q-disturbance to output transfer function of figure 6 is not exactly at 2100Hz.

Figure 10 shows the trajectory of the reference and the output voltage with and without observer in the 3D space using the -coordinate transformation. In both cases a single phase ohmic load of 5A was applied. All system relevant parameter are listed in the table 1.

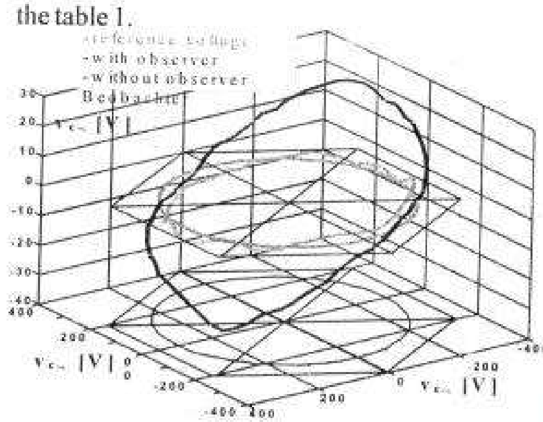

Figure: 10 3DRepresentation of the measured output with and without observer with ohmic load of 5A

TABLE I SYSTEM PARAMETER

Output voltage	v_C	230	V_{RMS}
Net Frequency	f_N	50	Hz
DC-link voltage	V_d	670	V
L-Filter	L	4	mH
C-Filter	C	60	F
C-DC-link	C_d	470	F
Switching frequency	f_s	9	KHz
Sampling period	T_d	333	s
Battery voltage	V_{Bat}	160	V

12. CONCLUDING REMARKS

In this paper, a three dimensional space vector modulation has been applied to the control of a 4-leg voltage source inverter model whish is deployed to invert the output of a stand-alone photovoltaic system. Load current has been estimated by a reduced order observer while the disturbance introduced by a non-linear load has been cancelled by a feedforward disturbance controller. Both experiment and simulation results have been deployed to show the emergence of stable system with about 16% higher utilization of the DC link voltage. With headwave eliminated for load current measurement, the resulting system which is implemented on a microcontroller has been found to be cheaper, simpler and more efficient than the existing ones.

13. REFERENCES

1. R . Kaasekc and E. L. Meyer "On the design and performance of stand alone PV systems" International Conference on Power System Planning & Operations (ICPSOP 2007) Cape Town South Africa pp. 28 36, Jan. 2007.

2. R. Kaseke and E. L. Meyer, "PV power system sizing for information and communication devices in schools outside the utility grid" WREC, Italy, August 2006 pp. 206 211.

3. L. Castener and S. Silvestre "Modelling Photovoltaic system using Pspice" John Wiley & Sons, England, 2002.

4. T. Sykora (Dispersed Electrical Energy Generation), Diploma thesis, FEE CTU, Prague, 2004.

5 J. A. Momoh, G. Boswell, "Value-Based Implementaion of Distributed Generation in Optimal Power Flow" North American Power Symposium (NAPS) 2005 Vol. 2, pp. 808 813.

6. Said El-Barbari, W. Hofmann, "Digital Control of a Three Phase 4 Wire PWM Inverter for PV Application". EPE '99, Lausanne, CD-ROM.

7. Said El-Barbari, W. Hofmann, " Digital Control of a Four Leg Inverter for Standalone Photovoltaic Systems with Unbalanced Load", IECON2000, Nagoya, CD-ROM.

8. U. Chukwu, B. Oni F. Kuate and E. Overton, "Teaching Solar Energy Application Using In-House Developed Testbench". Proceedings of the 37th IEEE Southeastern Symposium on System Theory, March 2022, 2005, Tuskegee University, pp 346-351.

9. E. E van Dyke, EL Meyer, FJ Vorster, AWR Leitch, "Long-term monitorring of photovoltaic devices", Renewable Energy, Vol. 25, 2002, pp. 183-197.

9. EL Meyer and B Mapuranga, "The Effect of Temperature on the Performance of Photovoltaic Modules at Regulated Voltage", PVSE Conference, Shanghai, China, October 2005. pp. 1015 1020.

10. Youichi Ito and Shoichi Kawauchi, "Microprocessor-Based Robust Digital Control for UPS with Three -Phase PWM Inverter", IEEE Transactions on Power Electronics, Vol. 10, No. 2, March 1995, pp. 196-204.

12 Lohman, B. "Zur Störgroßenaufschaltung im Zustandsraum", Universität Bremen 1997, at http://siemens.phisik.uni-bremen.de/lohmann/papers/default.html